AD-A120 027 ROYAL SIGNALS AND RADAR ESTABLISHMENT MALVERN (ENGLAND) F/G 7/4
THE PHASE DIAGRAM CD-HG-TE.(U)
1982 A W VERE, D J WILLIAMS, J B MULLIN
UNCLASSIFIED RSRE-MEMO-3387 DRIC-BR-84602 NL

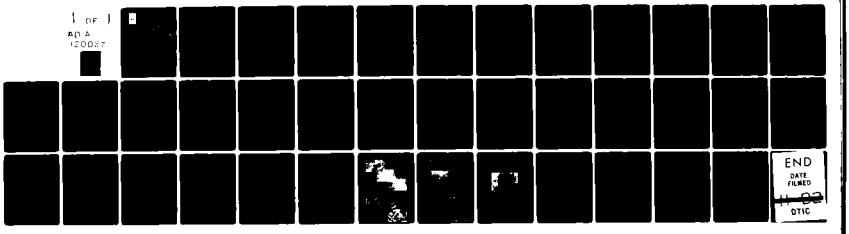

(2)

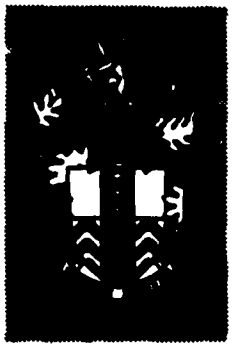

RSRE
MEMORANDUM No. 3387

ROYAL SIGNALS & RADAR ESTABLISHMENT

THE PHASE DIAGRAM Cd–Hg–Te

Authors: A W Vere, D J Williams
and J B Mullin

PROCUREMENT EXECUTIVE,
MINISTRY OF DEFENCE,
RSRE MALVERN,
WORCS.

ROYAL SIGNALS AND RADAR ESTABLISHMENT

Memorandum 3387

Title: THE PHASE DIAGRAM Cd-Hg-Te

Authors: A W Vere, D J Williams and J B Mullin

Date:

SUMMARY

This memorandum reports the results of a study of the published literature on the Cd-Hg-Te phase diagram and adds some further data from RSRE studies of the microstructure of alloys from the Te-rich carrier of the ternary phase diagram.

Where possible, attempts have been made to assess the relative merits of the data and to indicate the preferred result in cases where severe discrepancies appear between the various author's results.

For ease of reference the thermodynamic data available have been converted to standard values and summarised in tabular form.

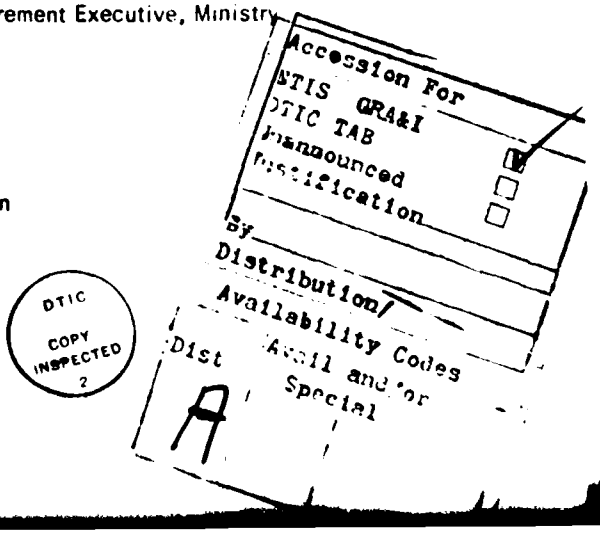

A

RSRE MEMORANDUM 3387

THE PHASE DIAGRAM Cd-Hg-Te

A W Vere, D J Williams and J B Mullin

LIST OF CONTENTS

1 INTRODUCTION

Compositions $Cd_xHg_{1-x}Te$ in pseudo-binary system HgTe-CdTe are becoming increasingly important infra-red detector materials. Part of this importance stems from the fact that the bandgap of the material (and hence its wavelength response) can be tuned by varying the cadmium concentration, Cd_x.

Initially, growth of this material was by the Bridgman technique, for which a knowledge of the phase relationships and segregation coefficients in the pseudo-binary section CdTe-HgTe is sufficient. In consequence, much of the early work on phase equilibria in the Cd-Hg-Te system concentrated on this section. More recently however, other growth techniques such as solution growth and 'Cast Recrystallise Anneal' (CRA) processes have been adopted. These require a more detailed knowledge of the full ternary system.

In this paper we attempt to summarise the known data on the Cd-Hg-Te phase diagram and to add some previously unpublished work from our own research. In view of the experimental difficulties involved in determining temperatures and vapour pressures in a highly volatile system exhibiting a marked degree of supercooling many of the published data are, at best, unreliable. The extent of these difficulties can be judged from the fact that the vapour pressure P_{Hg}

over $Cd_{0.2}Hg_{0.8}Te$ at its melting point (790°C) is approximately 30 atmospheres, but rises to about 90 atmospheres in the presence of excess free Hg mercury. Additionally, up to 50°C supercooling prior to solidification has been observed in some Te rich compositions.

2 TEMPERATURE - COMPOSITION RELATIONSHIPS - THE (T,x) DIAGRAM

In discussing the Cd-Hg-Te diagram we shall refer frequently to the structures of the vertical sections whose intersections with the basal plane are shown in figure 1. This diagram shows those sections for which published experimental data are available. The first and most commonly cited of these is the HgTe-CdTe pseudo-binary. (Figure 2.)

Several determinations of this section have been made, their marked differences serving only to emphasise the experimental difficulties outlined above. Early work by Woolley and Ray[1] using X-ray techniques confirmed that full solid solubility exists across the whole $Cd_xHg_{1-x}Te$ section of the ternary system. They also measured the lattice parameter of the alloy as a function of composition. The liquidus and solidus lines were also derived by Ray and Spencer[2] using differential thermal analysis measurements made on small (approx 1 gm) encapsulated samples. They differ widely however from those determined by Harman[3] and from the earlier liquidus measurements of Blair and Newnham[4].

The first attempt to reconcile these differences was made by Schmit and Speerschneider[5] whose pressure-temperature (P,T) diagram indicated a pressure dependence of the liquidus and solidus slopes and of the segregation coefficient. By postulating that the various authors' (T,x) diagrams had been constructed at different vapour pressures they were able to fit their data to all the results for the solidus and liquidus points for the composition $Cd_{0.2}Hg_{0.8}Te$. As we shall see in section 3 though, there is also some doubt as to the accuracy of Schmit and Speerschneiders' liquidus and solidus determinations. Steininger[6], for example, records a marked pressure dependence of the solidus at pressures up to 40 atm and his data for the (P,T) curve correspond more closely to Blair and Newnhams' determination of the liquidus line in the (T,x) diagram. The relative merits of the (P,T) diagrams will be discussed further in section 3 but so far as the pseudo-binary diagram is concerned it is only possible to conclude that failure to correct for Hg loss in establishing the equilibrium vapour pressure, or failure to allow sufficient time for equilibrium to be achieved, resulted in gross inaccuracies in some of the early phase diagram

determinations. The most reliable data appear to be those indicated by the solid lines in figure 2.

Although early work was confined to the pseudo-binary system, Bartlett Beans and Ellen[7] recognised that failure to control the Hg partial pressure adequately led to the precipitation of free tellurium and, by deliberately adding excess tellurium to HgTe, showed that there was a distinct correlation between the tellurium content and the occurrence of a mosaic cellular structure in the resulting crystals.

This departure from the pseudo-binary line becomes even more pronounced as the solidification rate is increased and more recent studies of growth techniques based on Cast Quench Anneal (or, to use the less tautological description, Cast Recrystallise Anneal, CRA) technique have demanded a wider knowledge of the ternary system. This is true also of the increasing attention now being paid to growth of $Cd_xHg_{1-x}Te$ alloys from Te-rich or Hg-rich solutions, which requires knowledge not only of the phases within the ternary field, but also of the slope of the liquidus surfaces and the location of the tie lines dictating the relationship between source composition and that of the deposited solid.

In order to form some idea of the general layout of the ternary diagram it is necessary to consider briefly the three constituent binary systems Cd-Hg Hg-Te and Cd-Te. Data on Cd-Hg[8] (fig 3) is sparse and of limited value. Two peritectics have been recorded, the first at 188°C and approximately 70% Cd and the second at -34°C at the extreme Hg-rich end of the diagram. At the Cd-rich end of the diagram an α-Cd solid solution is stable from the melting point of Cd (321°C) to below room temperature and shows a maximum Hg solubility of slightly over 20%. The ω-phase, formed by the peritectic reaction at 188°C is reported to be a b.c.t. structure. Opinions differ on its composition range the most generally accepted being 35-85% at room temperature. Claeson et al[9] have reported a transformation at around -14°C.

The Hg-Te diagram (figure 4) is taken from Hansen[10] with additional liquidus data from Brebrick and Strauss[11]. The diagram has been reviewed by Harman[3] in some detail. The chief features are the HgTe compound (mpt 670°C) occurring at the 50% Te composition and a eutectic point at 411°C: 85% Te. Delves[12] has suggested the occurrence of a monotectic at approximately 52% Te (inset fig 4) resulting from the presence of two immiscible liquids.

The Cd-Te phase diagram shown in fig 5 is essentially that derived by de Noble[13] Lorenz[14] and Kobayashi[15] showing the CdTe compound at the 50% Te composition (Tmpt = 1092°C) and two eutectic lines, the first at 321°C over the composition range 0-50% Te and the second at 437°C over the composition range 50-100% Te. Recent work by one of the present authors[16] has shown the existence of a eutectic on the Te-rich side, with a Te composition of approximately 98% suggesting that the diagram should be modified according to the broken line shown in fig 5.

These three binary diagrams can be combined to produce the elementary Cd-Hg-Te diagram. For the sake of clarity we will divide the ternary along the HgTe-CdTe pseudo-binary line and draw the Te-rich and Cd-Hg rich regions in separate diagrams. (Figs 6 and 7.)

The most immediately obvious feature of the Cd-Hg rich part of the diagram is the rapid rise in liquidus temperature as the composition becomes increasingly Te and/or Cd rich. The practical significance of this for solution growth experiments involving Hg-rich sources is that growth temperatures would have to be controlled to better than 1°C over the whole source and substrate region to avoid solid composition variations in excess of 0.2 atomic percent (a typical infra-red detector material specification). This fact, together with the low solubility of $Cd_xHg_{1-x}Te$ in Hg and the high vapour pressures involved (see section 2) makes this side of the pseudo-binary an unattractive starting point for LPE growth. The published data on the phase fields within the Hg-HgTe-CdTe-Cd region are restricted to a determination of the Hg rich end of the Hg-CdTe section by Vanyukov et al[17], who reported a very low solubility of CdTe in Hg (< 1%) and an observation by Gillham and Farrar[18] that annealing $Cd_xHg_{1-x}Te$ in a mercury over-pressure led to the formation of second phase closely related to the previously observed ω-phase, suggesting an extensive ω field penetrating deeply towards the HgTe-CdTe line in the Hg-HgTe-CdTe-Cd region of the ternary diagram.

The Te-rich side of the phase diagram, ie Te-CdTe-HgTe, is of greater practical significance and has therefore been the subject of greater experimental attention. Harman[19] and Ueda et al[10] have published data on the slope of the liquidus on the Te rich side (fig 8) for Te-$Cd_xHg_{1-x}Te$ sections of constant Cd:Hg ratio ranging from 0 to 0.2.

Care must be taken in comparing the two sets of data, since Ueda expresses composition in terms of $(Cd_xHg_{1-x})_{1-z}Te_{1.0}$, whereas Harman uses the more

conventional notation $(Cd_xHg_{1-x})_{1-y}Te_y$. The derived relationship $y = 1/(2 - z)$ must therefore be applied to convert Ueda's data to the conventional notation. When this is done it is found that the slope of the liquidus is the same in each case but that the actual temperatures differ by roughly 10-20°C. A recent investigation by Schmit[21] gives values close to those obtained by Harman although, as he points out, the composition data are not corrected for Hg-loss and do not therefore represent equilibrium values. The effect of this is to make the true compositions more Cd and Te rich than shown in the graphs of figure 8, displacing them towards the right. The larger discrepancy between Harman's and Ueda's data when compared to that between Harman's and Schmit's is consistent with a higher Hg-loss in Ueda's higher temperature growth process. No details of any correction for this loss are given in either Ueda's or Harman's paper.

The shape of the isothermal sections derived from the above data (fig 10) at temperatures in the region 500-700°C is interesting since they are concave with respect to the CdTe-HgTe section, whereas at higher temperatures the shape of the Hg-Te and Cd-Te liquidus lines would indicate a convex isothermal section in the intermediate field. The transition from convex to concave occurs in the region of 600°C (Ueda's data). The concavity of the surface at lower temperatures appears to be related to the presence of the Te-rich solid solution extending to the Te-rich side of the HgTe-Te eutectic. Extrapolation of Harman's data to intersect the Cd-Te binary would produce a slightly lower liquidus than the published data, consistent with the presence of a CdTe-Te eutectic at approximately 2% Cd. The projection is then expected to be as shown by the broken line in fig 1. Alloy compositions just to the right of this line represent the lowest melting point alloys from which $Cd_xHg_{1-x}Te$ can be precipitated and we have therefore made a more detailed metallographic study of this area of the phase diagram in an attempt to locate the position of the valley line joining the two binary eutectic points.

The required metallographic specimens were produced by casting. Specimens of constant Te composition, $(Cd_xHg_{1-x})_{0.2}Te_{0.8}$ and constant Cd:Hg ratio $(Cd_{0.2}Hg_{0.8})_{1-y}Te_y$ were chosen. The compositions of these are indicated by the filled circles in fig 1. The microstructures observed (figs 11 and 12) all show a eutectic, together with primary phase Te or $Cd_xHg_{1-x}Te$ according to the direction of the deviation from the eutectic point. No other phases were observed.

The composition of each specimen was determined by atomic absorption spectroscopy. In attempting to correlate the observed microstructures with the measured composition care must be taken to ensure that the equilibrium structure has been obtained. In $Cd_xHg_{1-x}Te$ ingots this is frequently difficult owing to the high degree of segregation and the combination of marked supercooling and a limited coupled growth[22] zone associated with the formation of the eutectic. Nevertheless by careful control of quenching rate it is possible to produce a fully eutectic structure of the type shown in fig 13 corresponding to a mercury telluride alloy containing about 83% tellurium, which is in reasonable agreement with values published elsewhere.

Microstructures of alloy compositions ranging from x = 0 to x = 1 for y = 0.8 (figure 11 a-f) all show a facetted primary phase, the composition of which varies from HgTe in the x = 0 alloy to CdTe in the x = 1 alloy. Overshoot of the eutectic composition as the alloy solidifies leads to secondary precipitation of Te in the form of an irregularly shaped lighter coloured phase. Finally the residual liquid composition reaches the coupled growth zone and undergoes eutectic solidification to form the darker background phase in the microstructure. High magnification examination of this eutectic shows it to be composed of a light-coloured Te phase combined with a darker phase, the composition of which varies from HgTe in the x = 0 alloy, through $Cd_xHg_{1-x}Te$ compositions of increasing x value to CdTe in the x = 1 alloy.

The occurrence of a CdTe/Te eutectic in the Cd-Te system has not previously been reported, but it is clear from atomic absorption analyses of Te rich compositions that the cadmium concentration in the eutectic lies between 1 and 2 atomic percent.

Figure 12 (a to e) show microstructures obtained from compositions along the line $(Cd_{0.2}Hg_{0.8})_{1-y}Te_y$ for y = 0.75; 0.80; 0.85; 0.90 and 0.95. An irregular dendritic primary phase $(Cd_xHg_{1-x})_{1-y}Te_y$ is observed for compositions $\leq Te_{0.85}$, but is replaced by primary Te-rich solid solution in the 0.90 and 0.95 alloys. Examination of the darker phase of the eutectic from the $Te_{0.90}$ and $Te_{0.95}$ compositions using SEM and EDAX techniques indicated that a true $(Cd_xHg_{1-x})_{1-y}Te_y$-Te eutectic was observed only in the surface region of the ingot ie in the first material to solidify. As solidification progressed, the Cd_x content of the lighter phase of the eutectic reduced to zero, so that the bulk of the ingot contained HgTe-Te eutectic. This segregation suggests that the eutectic valley line joining the HgTe-Te and CdTe-Te eutectics bends

sharply upwards in temperature as x approaches 1.0 and bends towards the Hg-Te axis as y decreases as shown in fig 1.

Having located the region of the diagram from which it is possible to achieve solution growth at temperatures low enough to produce controllable epitaxy and minimise interdiffusion between substrate and epilayer it is necessary to establish details of the segregation coefficient and the liquidus-solidus tie lines in the ternary diagram. Schmit's data on the lines for Te rich compositions close to the HgTe-Te eutectic (fig 9) emphasise clearly the major problem in attempting LPE growth of CMT since compositions differing by less than 5 at% in Hg content yield solid $Cd_xHg_{1-x}Te$ compositions ranging over 10 at% in Cd_x. To achieve the previously cited control on Cd_x value requires that the melt composition be controlled to within 0.02 mol% Hg. Using Harman's data from the (T,x) curve in fig 8 indicates a $\Delta x/\Delta T$ value of 0.1 mol% $^{o}C^{-1}$ corresponding to a required temperature stability of better than 0.2°C. The above calculation does not take into account diffusion in the solid state (though it is also true that neither do Schmit's experimental data on the tie lines and segregation coefficient) and therefore indicate a worst case situation.

3 THE PRESSURE-TEMPERATURE (P,T) DIAGRAM

Many of the problems encountered in the growth and application of $Cd_xHg_{1-x}Te$ arise from its dissociation at moderate temperatures. Time dependent changes in materials with unpassivated surfaces have been observed at temperatures only a few degrees above room temperature. Farrow et al[23] have studied the vaporisation of $Cd_xHg_{1-x}Te$ and also the end member constituents CdTe and HgTe using both Knudsen effusion and Langmuir techniques. They showed that the dissociation rate is controlled by the dissociation of HgTe (fig 14). At temperatures below 210°C Hg was the only detected vapour species. This led to a build up of the surface Te concentration and a consequent time dependent reduction in the Hg vapour flux J_{Hg}. Between 210°C and 320°C the Te effusion rate, J_{Te} increased towards a limiting value of $J_{Hg} = 2J_{Te_2}$. Above 320°C the two species are lost in the stoichiometric ratio leaving a porous surface film of CdTe.

Under the equilibrium conditions however the partial pressure of tellurium p_{Te} is four to five orders of magnitude lower than that of Hg. For this reason pressure-temperature diagrams for the HgTe-CdTe section of the ternary system are usually computed on the assumption that p_{Te} and p_{Cd} can be neglected.

Data from several authors' work on the (P,T) diagram for various $Cd_xHg_{1-x}Te$ compositions are shown in fig 15. There is general agreement in the literature on the data for the mercury vapour pressure over liquid Hg. Steininger's data[6] can be fitted to

$$\ln p_{Hg} = -\frac{7,149}{T} + 11.270 \qquad (516\text{-}798^{\circ}C) \qquad (1)$$

(where p_{Hg} is the partial pressure of mercury and T is the temperature in $^{\circ}K$) whilst those derived by Brebrick and Strauss[11] obey the relationship

$$\ln p_{Hg} = -\frac{7,092}{T} + 11.262 \qquad (333\text{-}657^{\circ}C) \qquad (2)$$

The average value of the heat of vaporisation of Hg derived from these equations is 14.14 kcals gm $atom^{-1}$ which is in reasonable agreement with the generally accepted literature value of 13.99 kcal gm $atom^{-1}$ [24].

There is general agreement too on the form of the three phase loop defining the envelope of p_{Hg} and temperature over which the condensed $Cd_xHg_{1-x}Te$ phase is stable. The occurrence of the loop indicates that the phase has an extended composition range over which the ratio of metal sub-lattice ions (A sites) to tellurium sub-lattice ions (B sites) varies, whilst the Cd:Hg ratio on the metal sub-lattice remains constant. The upper line bounding the loop therefore represents the p_{Hg} against 1/T relationship for mercury vapour in equilibrium with an alloy containing the maximum permissible concentration of A-type ions, ie the mercury-saturated solidus. In a similar manner, the lower boundary of the loop is defined as the tellurium-saturated solidus.

In general, the shape of the loop alters little with increasing Cd_x concentration in the alloy, but is displaced progressively towards higher temperatures and pressures as Cd_x increases from 0 to 40%. However, although all the authors' data show an extended near-vertical section of the curve in the region of the melting point, that derived by Schmit and Speerschneider extends over a much wider pressure range. Their experimental determination of the (P,T) diagram involved the measurement of heating and cooling curves whilst changing the $Cd_xHg_{1-x}Te$ sample temperature but maintaining a constant mercury reservoir temperature (and hence, constant p_{Hg}). They recognised that at low p_{Hg} values, rapid decomposition of the $Cd_xHg_{1-x}Te$ sample would occur, limiting the technique to one melting/solidification cycle. (In fact they questioned the validity of even a single run at low p_{Hg}, since it was found

that Cd_x increased markedly during solidification.) This effect results in a large departure from the pseudo-binary section towards the Cd-Te edge of the ternary phase diagram. On the assumption that the Cd and Te losses are negligible compared with the Hg loss, the x value change quoted by Schmit and Speerschneider can be estimated to have produced a final composition of $(Cd_{0.23}Hg_{0.77})_{0.44}Te_{0.56}$. This composition lies well outside the single-phase loop and it is probable that observations of the microstructure would have revealed substantial amounts of precipitated tellurium. The observed independence of pressure is therefore probably attributable to the presence of a two-phase mixture. For HgTe at least, the sloping Te-saturated solidus derived by Brebrick and Strauss[11] has been corroborated by the recent results of Irvine and Mullin[25] from their vapour phase growth experiments.

Perhaps the most significant anomaly in compar. (P,T) data for alloys of different Cd_x is that the three-phase loop for C $Hg_{0.7}Te$ extends to higher temperatures and pressures than that for Cd_0 $.6Te$. However in the latter case, the optical density technique used by tz[26] has been used to produce solidus rather than liquidus data. The s. .dus point obtained (745°C) agrees reasonably well with those shown on the pseudo-binary diagram (figure 2). The corresponding liquidus point is approximately 890°C ($10^3/T$ = 0.86).

Despite the differences in detail between the (P,T) envelopes for the various compositions, there is general agreement that the partial pressure of mercury over Hg-saturated $(Cd_xHg_{1-x})_{1-y}Te_y$ approaches that of free mercury whilst p_{Hg} over Te-saturated $(Cd_xHg_{1-x})_{1-y}Te_y$ reduces even more rapidly as the temperature falls. Some indication of the nature of the interatomic bonding in a chemical solution can be obtained from the change in chemical activity of one component a_{Hg} with concentration [N]. The two parameters are related by the expression

$$\gamma_{Hg} = \frac{a_{Hg}}{[N]} \qquad (3)$$

where γ is the activity coefficient. For ideal solutions γ remains constant over the whole composition range whereas in systems where one component, eg Hg, is only loosely bonded to the lattice, γ_{Hg} may increase rapidly as $[N_{Hg}]$ reduces. Steininger has observed that for compositions with y = 0.5 (ie stoichiometric) the activity of Hg, defined as

$$a_{Hg} = \frac{p_{Hg}^{CMT}}{p_{Hg}^{o}} \qquad (4)$$

where p_{Hg}^{CMT} is the partial pressure of Hg over the alloy and p_{Hg}^{o} is the vapour pressure of free Hg, is independent of both x_{Cd} and temperature (over the range 788-980°C), and obeys the relationship

$$\ln P(atm) = -\frac{7.149\ (^{o}K)}{T} + 10.206 \qquad (5)$$

This constant a_{Hg} value of 0.345 ± 0.020 and the consequent rise in γ_{Hg} as the [Hg] concentration reduces leads Steininger to propose a bonding model in which the solution is a mixture of strongly bonded CdTe molecules and dissociated or weakly bonded atoms Hg and Te. Addition of further Cd atoms displaces Hg to form further CdTe bonds. On the basis of this argument, the activity of the Hg depends not upon the cation ratio but on the availability of dissociated Te ie variations in the y value. The straight dotted lines in the liquid field region of fig 15 show a significant change in a_{Hg} as a function of y.

In contrast however, Vanyukov's data[27] for the solid solutions, take over a much lower and more restricted temperature range, (402-454°C) show a small but significant dependence of a_{Hg} upon x. (Figure 16.) The result of this is to produce an even steeper rise in γ_{Hg} as a function of increasing cadmium concentration than that observed in Steininger's work. Again however, Vanyukov et al conclude that the only possible explanation of this is based on the assumption that the CdTe bond is much stronger than the Hg-Te bond and is therefore formed preferentially as the Cd concentration is increased. The relevant activity coefficients are summarised in Table 1.

4 THERMODYNAMIC DATA FOR HgTe AND $Cd_xHg_{1-x}Te$

Once the partial pressures of the components in the system are determined the Gibbs free energy ΔG^{o} for the formation of the alloy can be derived from the relationship

$$\Delta G^{o} = RT \ln p_{Hg}^{(1-x)} \cdot p_{Cd}^{x} \cdot p_{Te}^{y} \qquad (6)$$

where x, 1-x and y are the mole fractions of Cd, Hg and Te respectively. For the binary alloy HgTe this reduces to

$$\Delta G^{o}\,[HgTe_{(g)}] = RT \ln p_{Hg}\, p_{Te}^{\frac{1}{2}} \qquad (7)$$

In this case the values of p_{Hg} are easily determined but the partial pressure of Te is much lower, particularly on the Hg-saturated solidus. Brebrick and Strauss found that the p_{Te} values here were only marginally above the detection limit of their optical density technique and the experimental data were supplemented by theoretical values calculated from the Duhem-Margules relationship between the component vapour pressures in a system. These computed p_{Te} values are indicated by the short vertical lines on the Hg-saturated solidus of figure 17.

Using the p_{Hg} and p_{Te} data obtained and considering the reaction

$$Hg_{(g)} + \frac{1}{2}\,Te_{2(g)} \rightleftharpoons HgTe_{(c)} \qquad (8)$$

they derived an expression for the Gibbs free energy ΔG^{o} of the form

$$\Delta G^{o}\,[HgTe_{(c)}] = -41.66 + 42.7\,(10^{-3})T \quad \text{kcal/mole} \qquad (9)$$

for the temperature interval 778-943°K. Converting the ΔH^{o} value of -41.66 kcals/mole to the room temperature value ΔH^{o}_{298} for the formation of $[HgTe_{(c)}]$ from $Hg_{(\ell)}$ and $Te_{(c)}$ gives a value of -9.6 kcals/mole (cf $\Delta H^{o}_{298}\,CdTe_{(c)} = -24.5 \pm 0.5$ kcals/mole[28]). Equation (14) also yields a value of $\Delta S^{o}_{298} = 26.7$ cals/mole/°C. These values of ΔH^{o} and ΔS^{o} show reasonable agreement with earlier values determined by Goldfinger and Jeunehomme[29]. However the data obtained by the latter are of somewhat dubious value as they were obtained from Knudsen effusion cell measurements taken at relatively high temperatures (300-400°C). Under these conditions the HgTe dissociation is dominated by a Te surface layer and the partial pressures derived are not measured under equilibrium conditions. The reasonable agreement obtained is therefore probably more attributable to the relative insensitivity of ΔH^{o} and ΔS^{o} to change in temperature as compared to ΔG^{o}.

Schwartz[26] has applied a similar analysis to the p_{Hg}, p_{Cd} and p_{Te} data obtained for $Cd_{0.414}Hg_{0.584}Te$, deriving a ΔG^{o} expression of the form

$$\Delta G^{o}\,[Cd_{0.414}Hg_{0.584}Te]_{c} = -52.93 + 42.18(10^{-3})T \quad \text{kcal/mole} \qquad (10)$$

$$0.584Hg_{(g)} + 0.416Cd_{(g)} + 0.500Te_{(g)} \rightarrow Hg_{0.584}Cd_{0.414}Te_{(c)} \quad (11)$$

If however the reaction is between the pseudo binary end-members HgTe and CdTe rather than the three elements, ie

$$0.584HgTe_{(c)} + 0.414CdTe_{(c)} \rightarrow Hg_{0.584}Cd_{0.414}Te_{(c)} \quad (12)$$

then the corresponding ΔG^{o} is of the form

$$\Delta G^{o}\left[Cd_{0.414}Hg_{0.584}Te\right]_{(c)} = -0.05 - 1.46(10^{-3})T \text{ kcal/mole} \quad (13)$$

in which $\Delta H^{o} \simeq 0$. This is analogous to the expression for an ideal solution in which ΔH_{m} the heat of mixing is zero and the entropy of mixing ΔS_{m} is given by

$$\Delta S_{m} = -R[(1-x)\ln x + x \ln x] \quad (14)$$

Again, the ΔS_{m} value of 1.35 cals/mole/^{o}C obtained from equation (14) agrees well with that of 1.46 cals/mole/^{o}C from equation (13) but, as Schwartz points out, the good agreement is somewhat coincidental. Nevertheless the thermodynamic data for the pseudo-binary suggest again the near ideality of the HgTe-CdTe solid solution. Details of several authors' data for the thermodynamic properties of HgTe and $Cd_{x}Hg_{1-x}Te$ alloys are given in Tables 1, 2 and 3.

5 SUMMARY

The collected data on the (T,x) and (P,T) relationships on the Cd-Hg-Te ternary system show general agreement on the type and extent of the phases observed in the system. The bulk of the data refers naturally to the most important section of the diagram for practical purposes, namely the HgTe-CdTe pseudo-binary section, but the recent interest in LPE growth has stimulated work on the Te-rich side of the diagram and, to a lesser extent the Hg-rich corner. Despite this the Hg-HgTe-CdTe-Cd area of the ternary system remains largely undefined. Whilst there is now some general agreement on the shape of the liquidus and solid lines for the $(Cd_{x}Hg_{1-x})_{0.5}Te_{0.5}$ system, the extent of the phase range towards the Hg-rich and Te-rich sides of the pseudo-binary line remains unresolved but has great practical importance in determining the point defect concentrations available and their effect upon the electrical properties of IR detector materials. The variations between the results

obtained by different authors provide a salutory lesson in the need for extremely close control of vapour pressure and hence temperature in practical growth systems.

6 ACKNOWLEDGEMENTS

The authors wish to thank their colleagues at RSRE for helpful discussion and criticism of the manuscript; in particular to Drs S Irvine and M Astles for their valuable comments and to Dr R Farrow for permission to reproduce figure 14. Thanks are also due to Dr J Schmit of Honeywell Technology Centre Minnesota for permission to reproduce the unpublished data of fig 9.

REFERENCES

1 J C Woolley and B Ray
J Phys Chem Sol 13 151 (1960)

2 B Ray and P M Spencer
Phys Stat Soc 22 371-372 (1967)

3 T C Harman
Physics and Chemistry of II-VI Compounds p 784
Interscience (1967)

4 J Blair and R Newnham
Metallurgy of Elemental and Compound Semiconductors 12
Interscience (1961)

5 J L Schmit and C J Speerschneider
Infrared Physics 8 p 247-253 (1968)

6 J Steininger
J Elect Mats 5 No 3 p 299-320 (1976)

7 B E Bartlett, J Deans and P C Ellen
J Mat Sci 4 266-270 (1969)

8 O J Kleppa
Acta Met 8 435-445 (1960)

9 T Claeson, H L Luo, T R Anatharaman, and M F Merriam
Acta Met 14 285 (1966)

10 M Hansen
Constitution of Binary Alloys p 840
McGraw Hill 1958

11 R F Brebrick and A J Strauss
J Phys Chem Solids 26 989-1002 (1965)

12 R T Delves
Brit J App Phys 16 343-351 (1965)

13 D de Noble
Philips Res Repts 14 488 (1959)

14 M R Lorenz
J Phys Chem Sol 23 939-947 (1962)

15 M Kobayashi
Z Anorg Chem 69 1 (1911)

16 D J Williams
To be published in J. Cryst. Growth

17 A V Vanyukov, I I Krotov and A I Ermakov
Neorganicheskie Materialy 13 No 5 p 667-671 (Eng Trans) 1977

18 C J Gillham and R A Farrar
J Mat Sci 12 1994-2000 (1977)

19 T C Harman
British Assocn for Crystal Growth Meeting on II-VI Compounds Lancaster 1980
(unpublished)

20 R Ueda, O Ohtsuki, K Shinohara and Y Ueda
J Cryst Growth 13/14 668-671 (1972)

21 J L Schmit - private communication based on data from AFWAL-TR-80-4068.

22 L M Hogan
J Aust Inst Metals 9 No 4 228-239 (1964)

23 R F C Farrow, G R Jones, G M Williams, P W Sullivan, W J O Boyle and
J T M Wotherspoon
J Phys D App Phys 12 L117-120 (1979)

24 R C West (Ed)
Handbook of Physics and Chemistry (51st Edition) D-56
The Chemical Rubber Co, Cleveland, Ohio (1970)

25 S J C Irvine and J B Mullin
J Cryst Growth - to be published (also presented at ECCG2 Lancaster Dept 1979)

26 J P Schwartz
PhD Thesis Marquette University 1977

27 A V Vanyukov, I I Krotov and A I Ermakov
Neorganicheskie Materialy 14 No 4 p 512-515 (Eng Trans)(1978)

28 O Kubaschewski, F Ll Evans, C B Alcock
Metallurgical Thermochemistry - Pergamon 1967, p 314.

29 P Goldfinger and M Jeunehomme
Trans Faraday Soc 59 2851 (1963)

30 E A Balagurova, N V Vladimirov, A A Ryazantsev, Yu K Tovpentsev and
E N Khabarov
Inorganic Materials 10 No 6 1135-1136 (1974)
Phase Diagram of the system HgTe-CdTe.

FIGURE CAPTIONS

1 Basal Plane of the Cd-Hg-Te ternary system showing binary and pseudo-binary sections for which (T,x) data are available. The hexagonal point indicates the composition $Cd_{0.2}Hg_{0.8}Te$ commonly used for infra-red detectors.

2 Liquidus and solidus data for the HgTe-CdTe pseudo-binary section. The solid lines indicate the most reliable data available.

3 The Cd-Hg binary phase-diagram (after Claeson et al[9]).

4 The Hg-Te binary phase-diagram (after Hansen[10] and Brebrick and Strauss[11]).

5 The Cd-Te binary phase-diagram (after de Noble[13] and Lorenz[14]).

6 The Te-HgTe-CdTe region of the ternary phase diagram.

7 The Hg-HgTe-CdTe-Cd region of the ternary phase diagram.

8 Liquidus lines on Te-CMT sections of the phase diagram for various Cd/Hg ratios. (□ after Harman[19] O after Ueda[20] ● after Schmit[21]).

9 Tie lines in the Te-rich region of the ternary system (after Schmit[21]).

10 Liquidus isotherms in the Te-CdTe-HgTe region of the ternary diagram. (⊖ Ueda et al[20]; □ Harman[19]).

11 Microstructures of $(Cd_xHg_{1-x})_{0.2}Te_{0.8}$ compositions with x = a) 0.0; b) 0.2; c) 0.4; d) 0.6; e) 0.8 and f) 1.0.

12 Microstructures of $(Cd_{0.2}Hg_{0.8})_{1-y}Te_y$ compositions with y = a) 0.75; b) 0.80; c) 0.85; d) 0.90 and e) 0.95.

13 Microstructure of the eutectic composition, $Hg_{0.17}Te_{0.83}$.

14 Dissociation vapour pressures over $Hg_{0.8}Cd_{0.2}Te$ X Hg; O Te_2; O Cd. The broken line represents the equilibrium vapour pressure of Hg over $Hg_{0.8}Cd_{0.2}Te$ (after Farrow et al[23]).

15 p_{Hg} v 1/T data for $Cd_xHg_{1-x}Te$ compositions.

16 p_{Hg} over Hg-saturated HgTe as a function of reciprocal temperature[17].

17 p_{Te_2} v 1/T data for HgTe (after Brebrick and Strauss[11] and Steininger[e]).

Activity Coefficients ($\gamma_{Hg} = a_i x_i$) for HgTe and $Cd_xHg_{1-x}Te$			
Composition x_{CdTe}	Liquid γ_{Hg} (Vanyukov[25])	γ_{Hg} (Steininger[6])	Solid γ_{Hg} (Vanyukov[25])
0.0	0.68	-	1.6
0.2	0.75	0.138	2.2
0.4	0.80	0.104	3.1
0.6	0.85	0.069	4.5
0.8	0.90	0.035	-

TABLE 1 Activity Coefficients for HgTe and $Cd_xHg_{1-x}Te$

Turn through 90^o and type as tables 2-5.

Material	$\log_e p_{Hg}$ (atmospheres)	Temp Range ^{o}K	Reference
$Hg_{(\ell)}$	$-\frac{7,149}{T} + 11.270$	789-1071	(6)
	$-\frac{7,092}{T} + 11.262$	606-930	(11)
	$-\frac{7,500}{T} + 11.84$	663-713	(17)
$HgTe_{(c)}$ (Hg saturated)	$-\frac{6,860}{T} + 10.85$	666-735	(11)
$HgTe_{(c)}$ (Te saturated)	$-\frac{23,217}{T} + 18.76$	735-845	(25)
$(Cd_xHg_{1-x})_{0.5}Te_{0.5(\ell,c)}$ ($x \approx 0$-0.6)	$-\frac{7,149}{T} + 10.21$	903-1253	(6)

TABLE 2 Equilibrium vapour pressure of mercury p_{Hg}(atm) over Hg, HgTe and $Cd_xHg_{1-x}Te$.

REACTION	ΔG° kcal/formula weight	Temp Range ^{o}K	Ref
1) $Hg_{(g)} + \frac{1}{2}Te_{2(g)} = HgTe_{(c)}$	$- 41.66 + 42.71(10^{-3})T$	778-943	11
2) $Hg_{(g)} + \frac{1}{2}Te_{2(c)} = HgTe_{(c)}$	$- 26.8 + 31.2(10^{-3})T$	435-555	29
3) $Hg_{(g)} + \frac{1}{2}Te_{2(g)} = HgTe_{(\ell)}$	$- 32.96 + 33.47(10^{-3})T$	778-943	6
4) $0.584Hg_{(g)} + 0.416Cd_{(g)} + 0.500Te_{2(g)} = Hg_{0.584}Cd_{0.416}Te_{(c)}$	$- 52.93 + 42.18(10^{-3})T$	830-920	26
5) $0.584Hg + 0.416Cd = Hg_{0.584}Cd_{0.416}Te_{(c)}$	$- 0.05 - 1.46(10^{-3})T$	830-920	26

TABLE 3 Standard free energies of reactions for the formation of HgTe and $Cd_xHg_{1-x}Te$

Material	Latent Heat of Vaporisation L_e (kcals $mole^{-1}$)	Heat of Formation $-\Delta H^{o}_{298}$ (kcals $mole^{-1}$)	Standard Entropy $-\Delta S^{o}_{298}$ (cals $mole^{-1}$ $^{o}C^{-1}$)	Reference
Hg	- 13.99 (365°C)			24
	- 14.21 (576-798°C)			6
	- 14.90 (333-657°C)			11
	- 14.60 (390-440°C)			27
	- 14.13			28
	- 14.09 (333-657°C)			11
	- 14.90 (390-440°C)			29
	- 23.0 (400-575°C)	(Te saturated)		25
Hg		0	18.2 ± 0.1	28
$Cd_{0.416}Hg_{0.584}Te$		20	27.2	26
CdTe		24.5 ± 0.5	22.4 ± 1.0	28

TABLE 4 Heats of vaporisation and formation and standard entropies for Hg, $Cd_{0.416}Hg_{0.584}Te$ and CdTe.

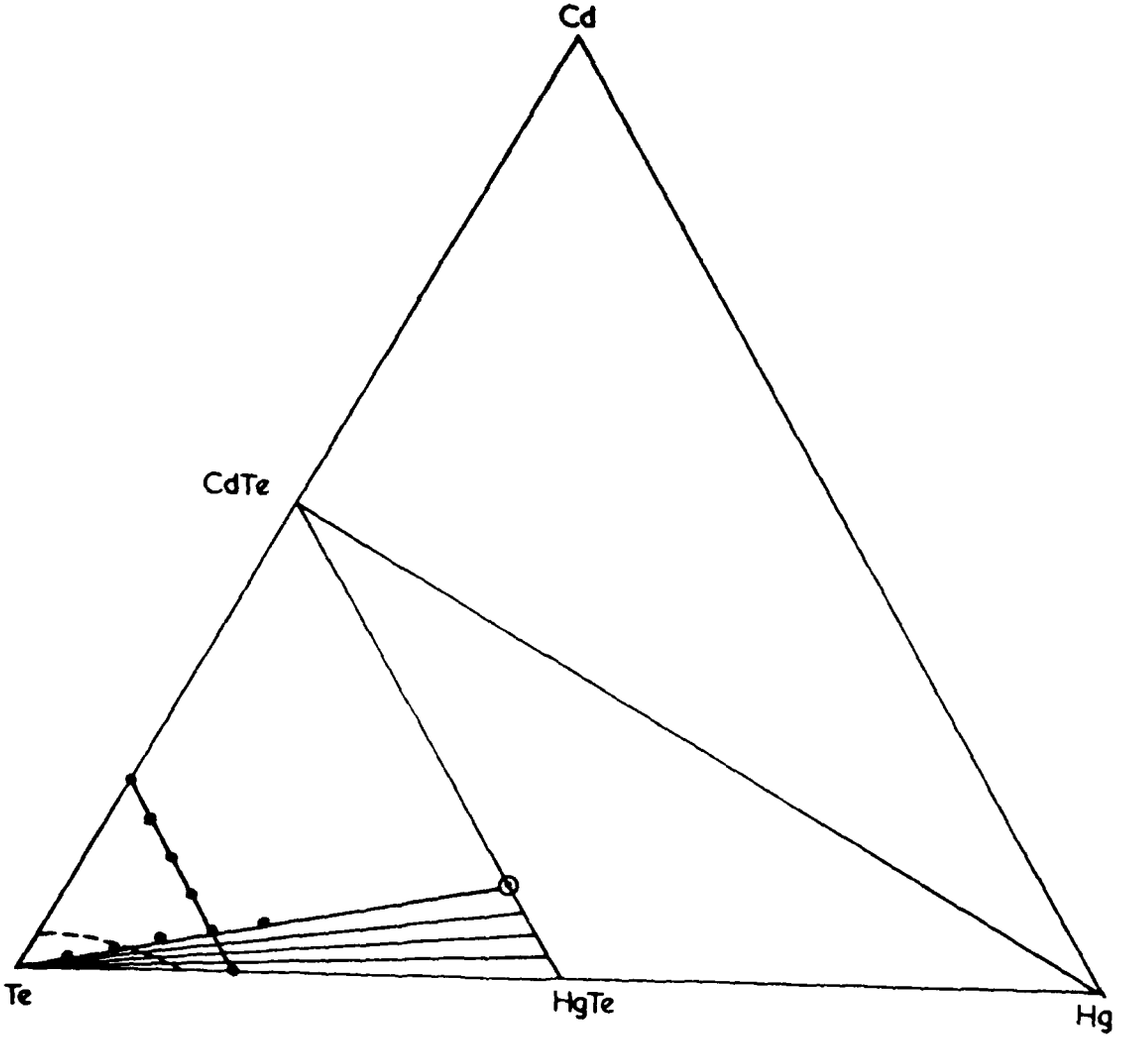

BASAL SECTION OF THE Cd-Hg-Te PHASE DIAGRAM SHOWING PRINCIPAL COMPOSITIONS AND SECTIONS INVESTIGATED

FIG 1

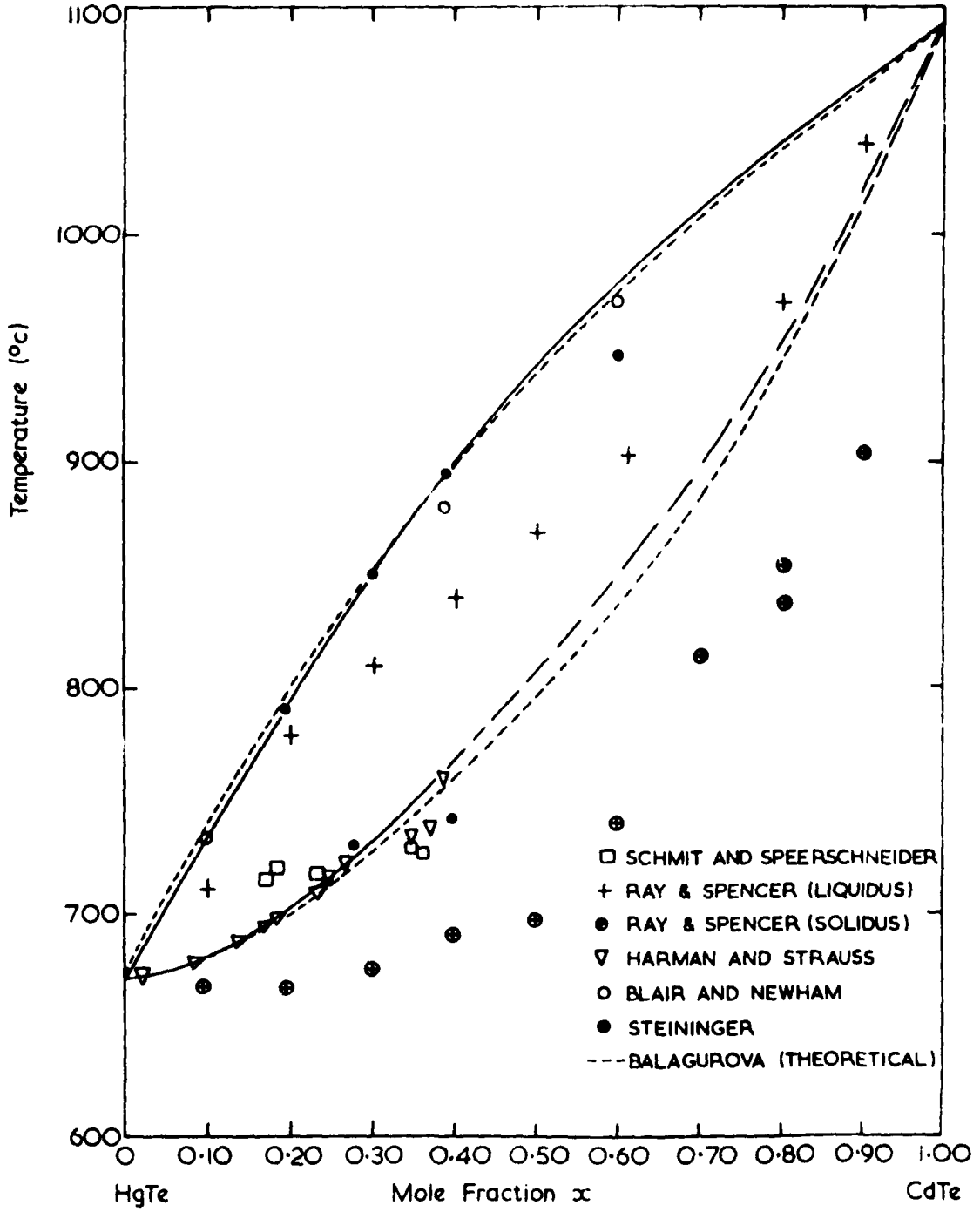

THE HgTe – CdTe PSEUDOBINARY PHASE DIAGRAM

FIG 2

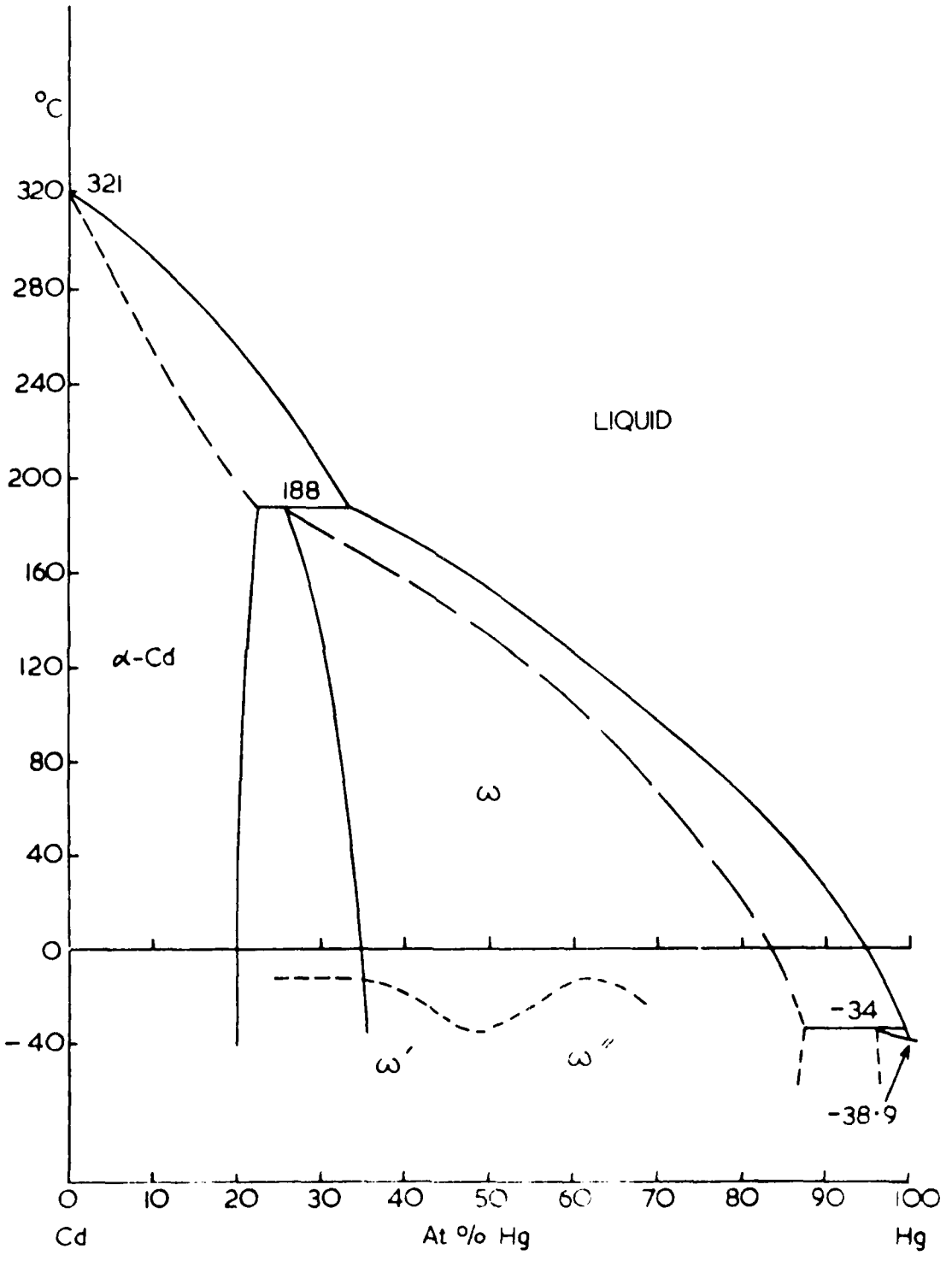

Cd-Hg PHASE DIAGRAM (after CLAESON et al [9])

FIG 3

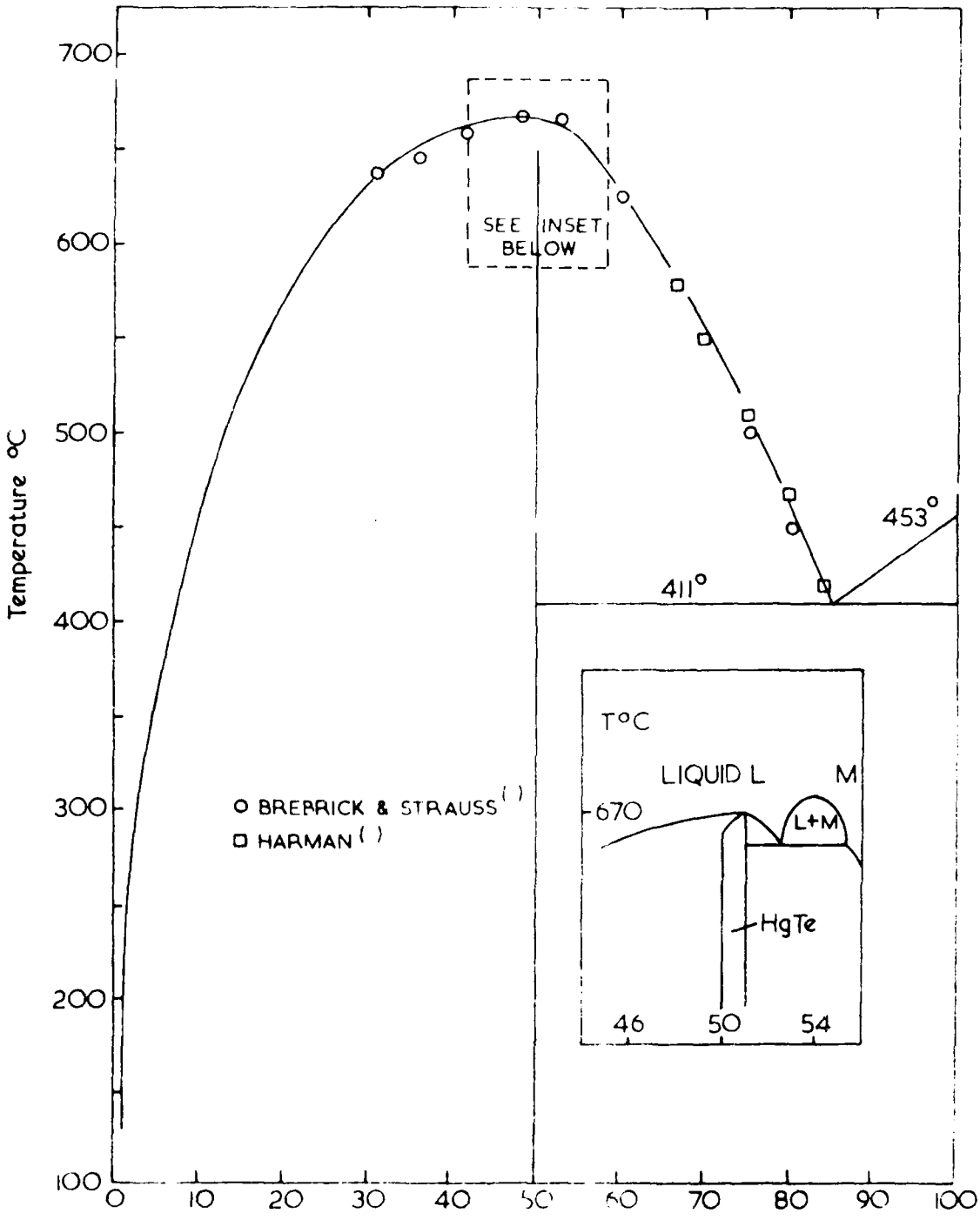
700
600
500
400
300
200
100
Temperature °C
0
10
20
30
40
50
60
70
80
90
100
SEE INSET BELOW
453°
411°
O BREBRICK & STRAUSS ( )
□ HARMAN ( )
T°C
LIQUID L
M
670
L+M
HgTe
46
50
54

FIG 4

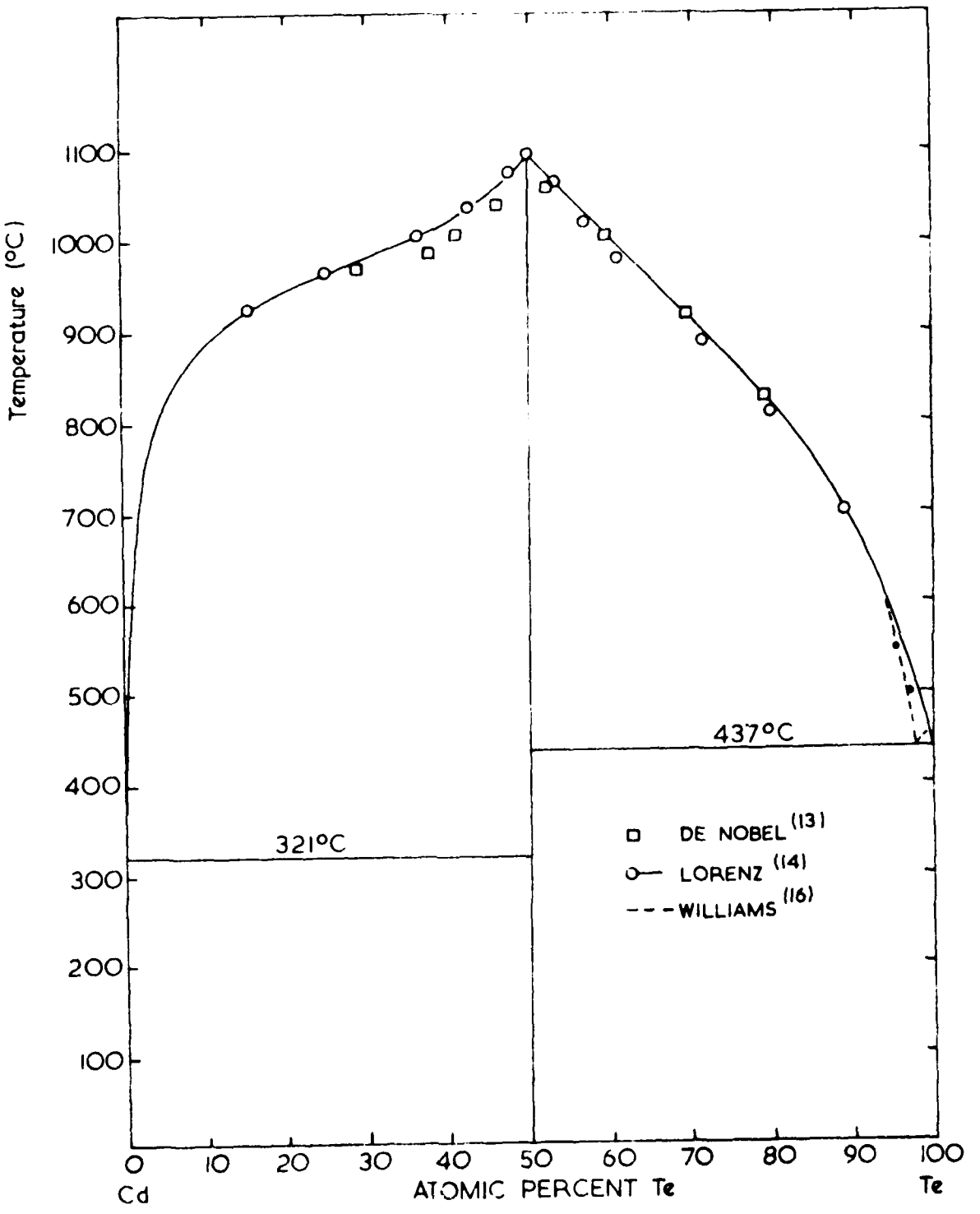

Cd-Te PHASE DIAGRAM

FIG 5

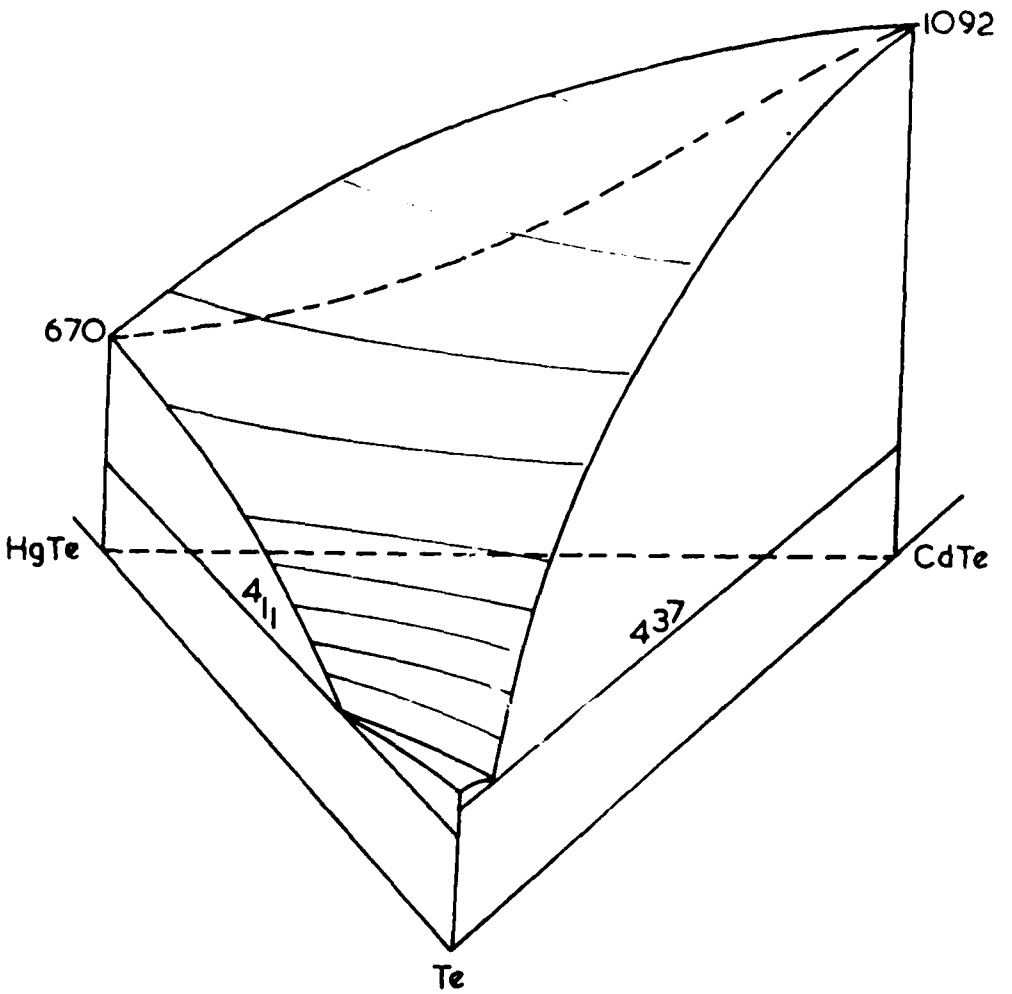

THE Te RICH CORNER OF THE Cd-Hg-Te PHASE DIAGRAM

FIG 6

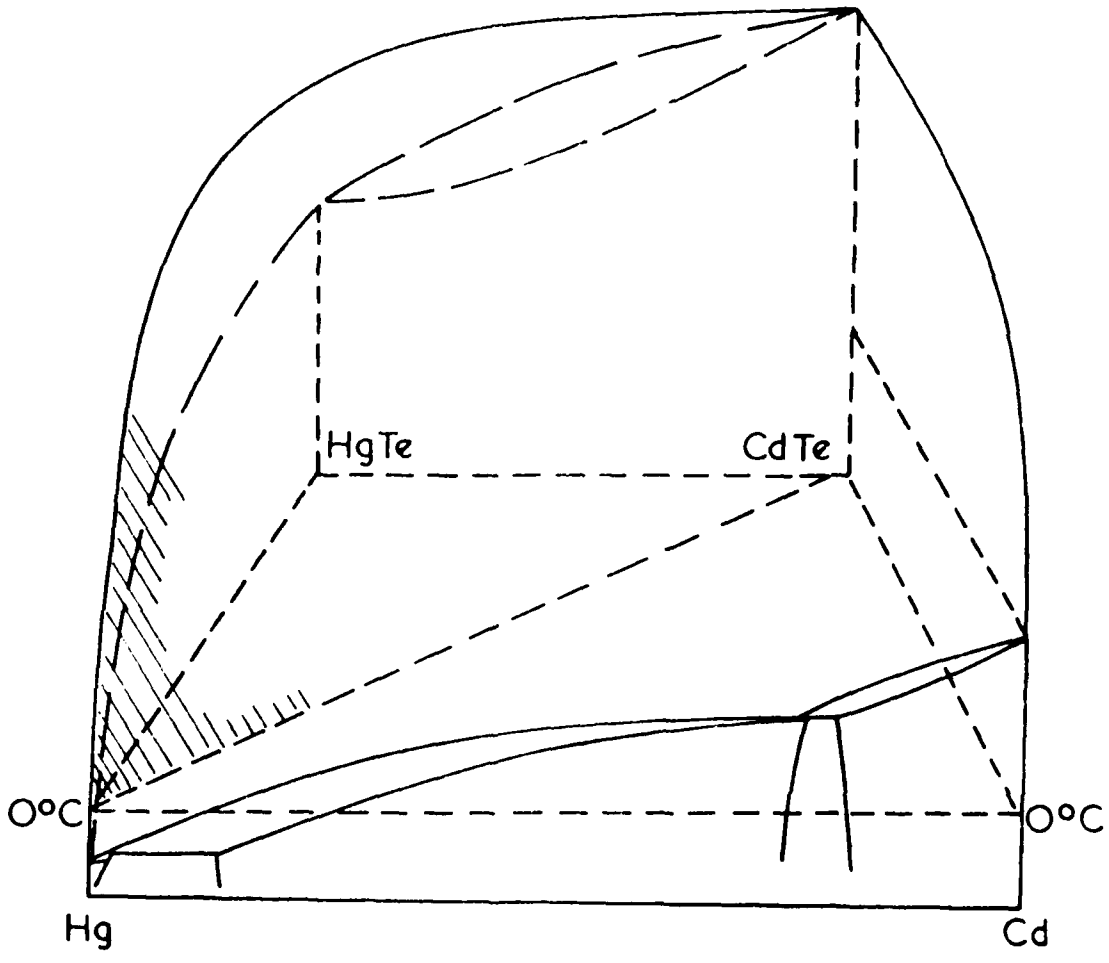

THE Hg-Cd SIDE OF THE Cd-Hg-Te PHASE DIAGRAM

FIG 7

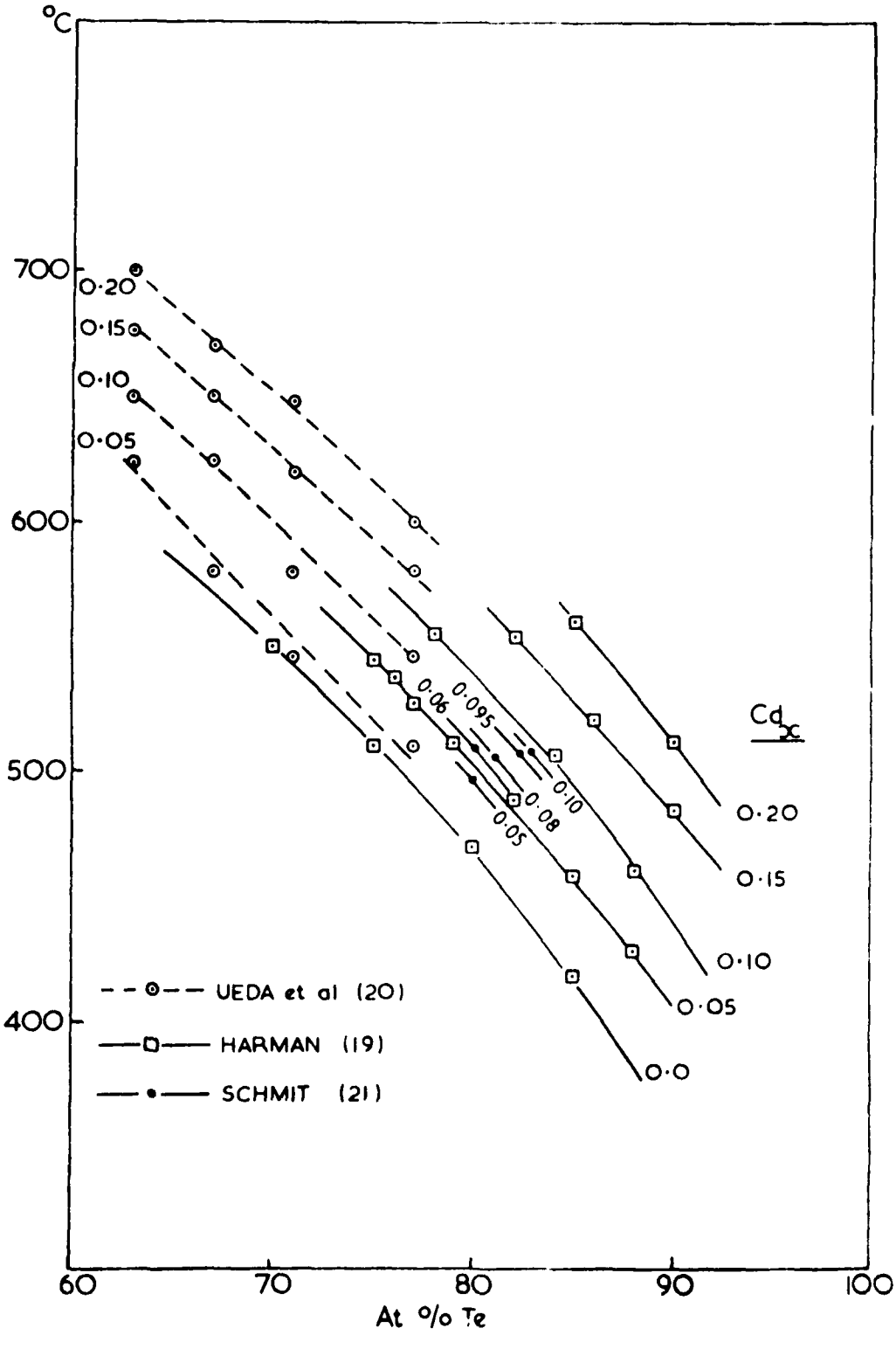

LIQUIDUS DATA FOR $(Cd_xHg_{1-x})_{1-y}Te_y$

FIG 8

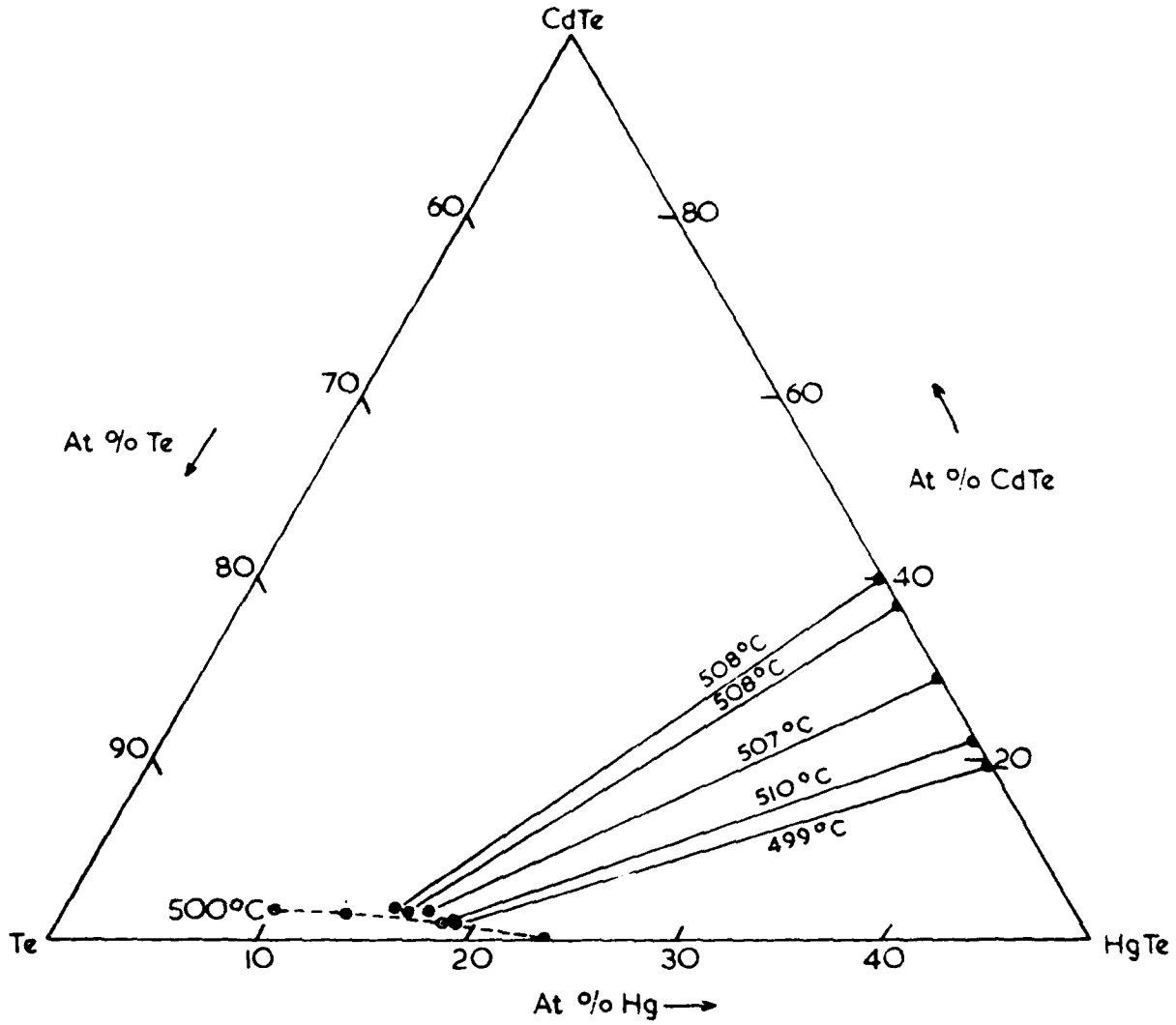

TIE-LINES ON THE Te-RICH SIDE OF THE Cd-Hg-Te PHASE DIAGRAM

FIG 9

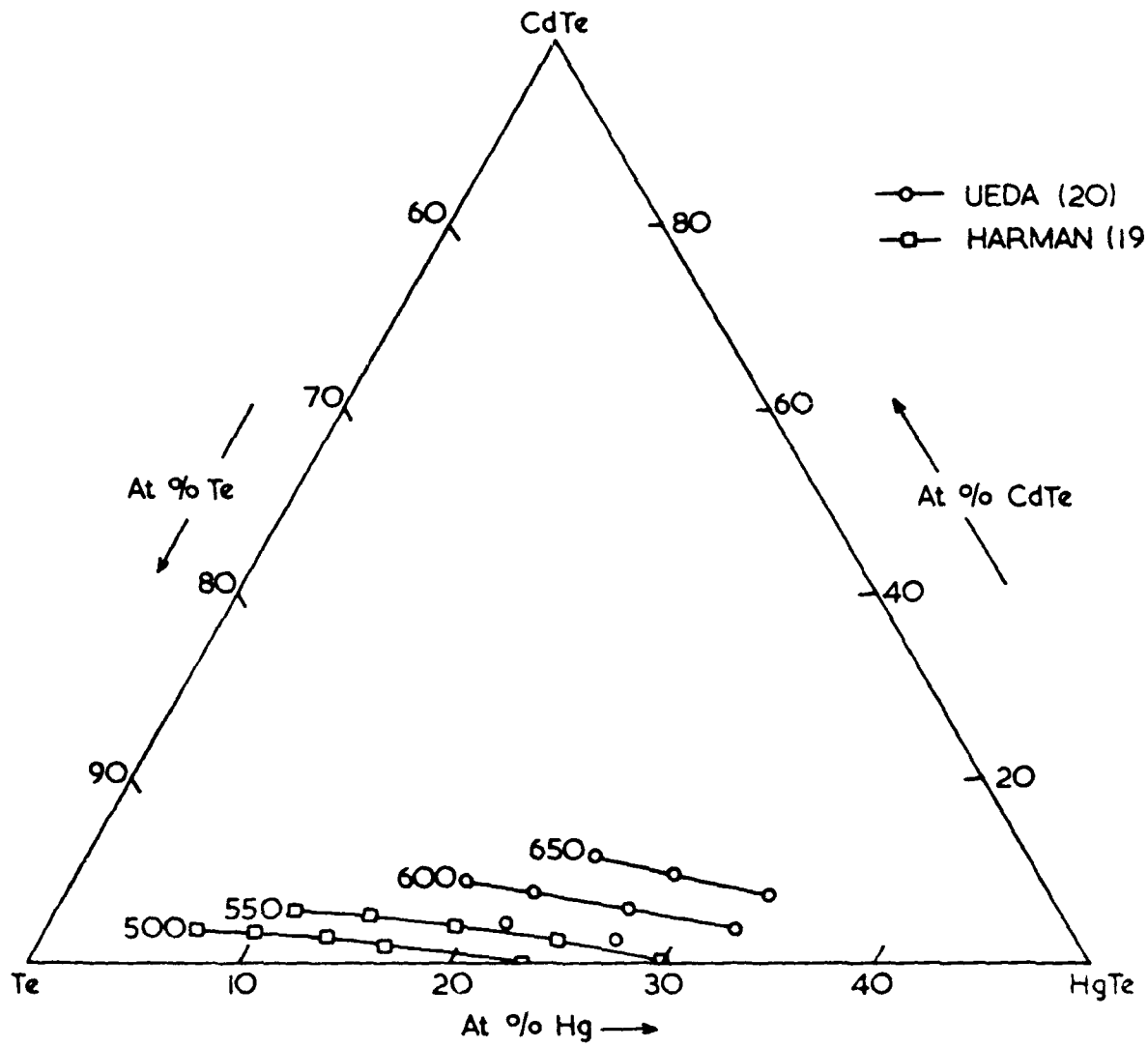

LIQUIDUS ISOTHERMS IN THE Te – HgTe – CdTe REGION OF THE PHASE DIAGRAM

FIG 10

FIG 11

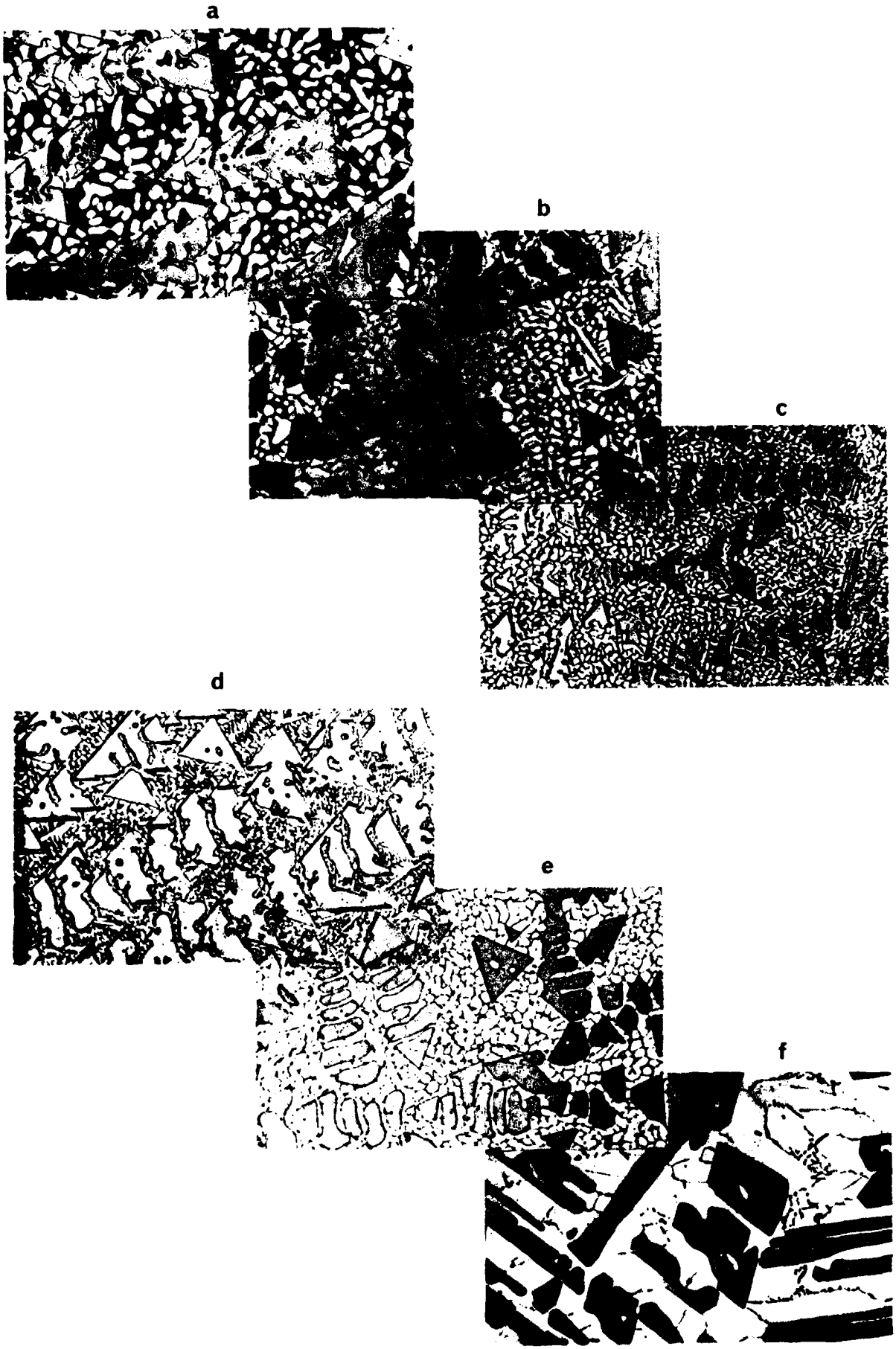

FIG 12

a

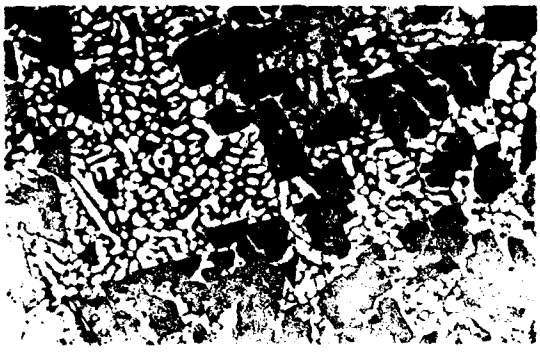

b

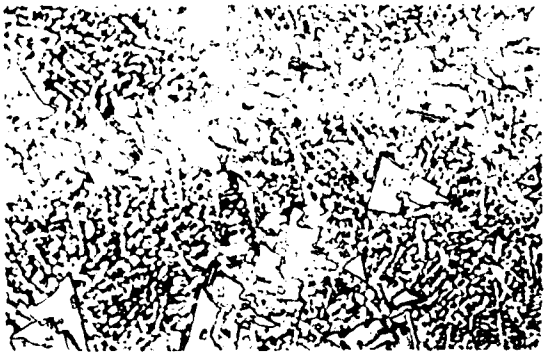

c

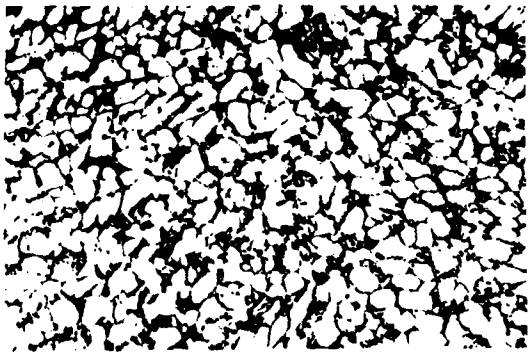

d

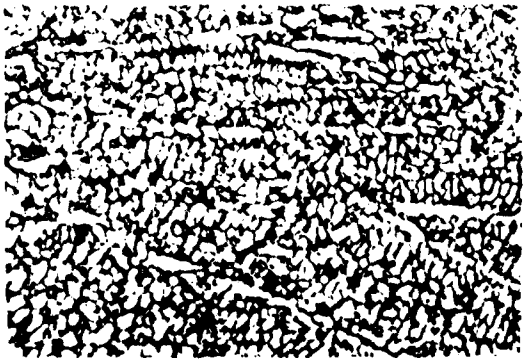

e

FIG 13

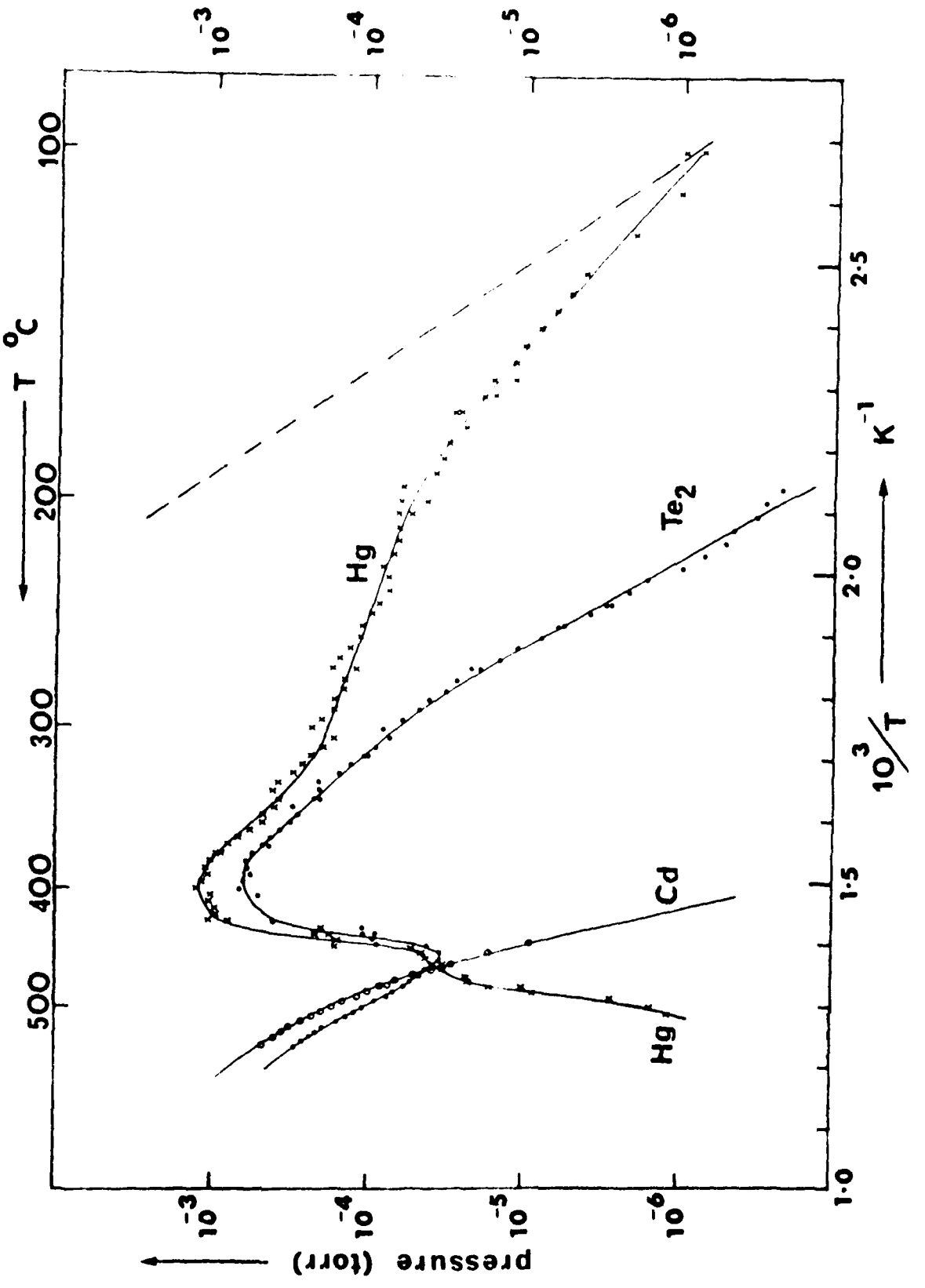
T °C
100
200
300
400
500
10^{-3}
10^{-4}
10^{-5}
10^{-6}
pressure (torr)
Hg
Te_2
Cd
Hg
$10^3/T$ K^{-1}
1·0
1·5
2·0
2·5

FIG 14

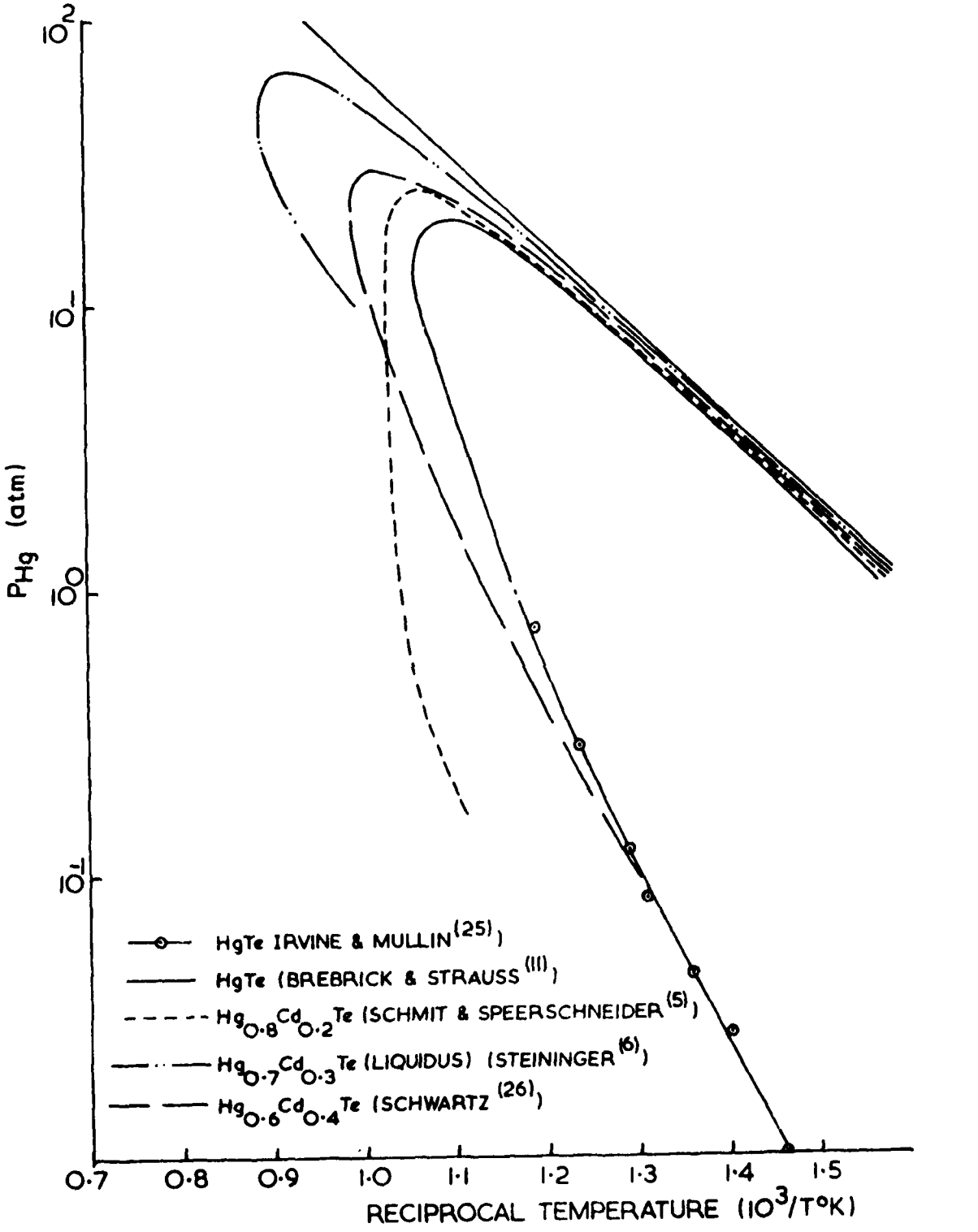

THE P–T DIAGRAM FOR VARIOUS $Cd_xHg_{1-x}Te$ COMPOSITIONS

FIG 15

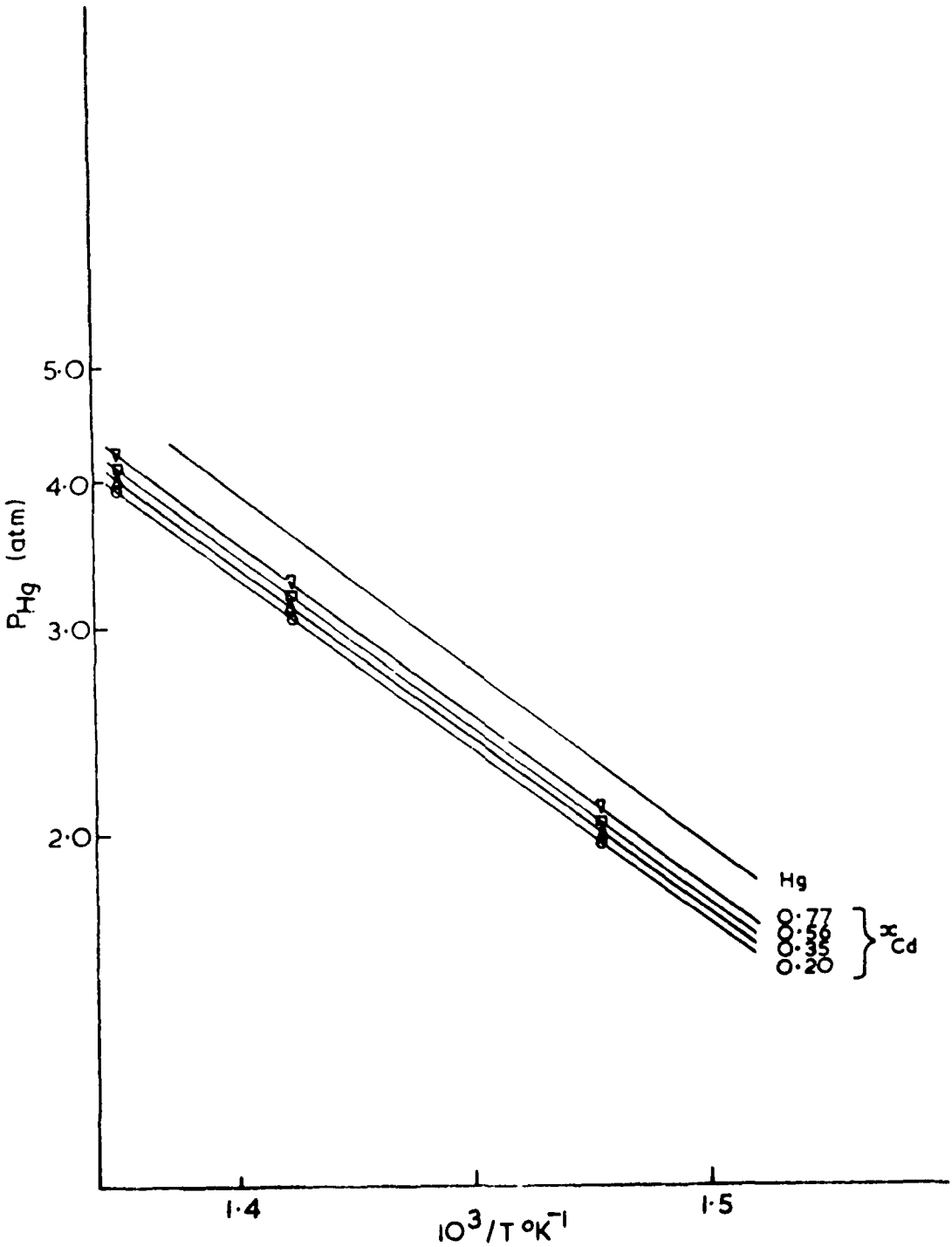

EXPANDED P_{Hg} v. $^1/_T$ PLOT FOR $^1/T = 1{\cdot}4 \times 10^{-3}$ TO $1{\cdot}5 \times 10^{-3}$

FIG 16

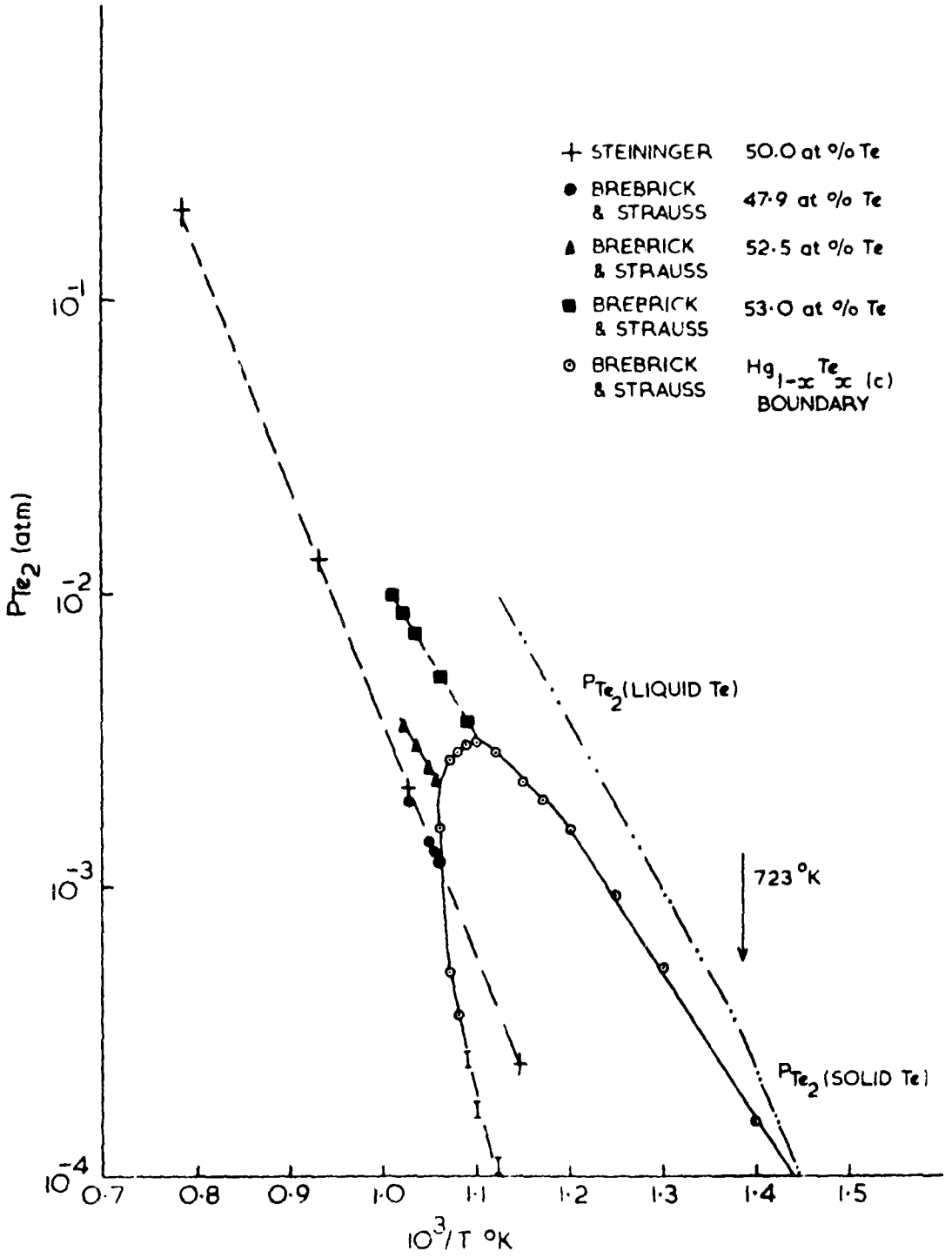

Te-VAPOUR PRESSURE DATA FOR $(Cd_xHg_{1-x})_{1-y}Te_y$

FIG 17

END

DATE
FILMED

DTIC